

Rheological behaviour of fresh cement paste as measured by squeeze flow

B. H. MIN*, L. ERWIN*, H. M. JENNINGS†

Departments of Mechanical Engineering Material Science and Engineering* Civil Engineering†, Robert R. McCormick School of Engineering and Applied Science, Northwestern University, Evanston, Illinois 60208, USA*

A method is proposed for measuring the rheology of cement paste under conditions that suppress shear flow, i.e. squeezing. This method is based on squeezing samples in a servohydraulic compression–tension testing machine, and is different from the commonly used shear flow experiments. Possible artefacts such as the buoyancy of the piston that penetrates the paste, sedimentation of cement paste, geometry of the container, and friction at the interface between the top plate (or piston) and sample are investigated. Plots of stress versus apparent strain were obtained and compared with results from standard shear flow experiments. Because cement paste has both viscoelastic and viscoplastic characteristics, results are analysed in terms of both solid-like deformation and liquid-like flow behaviour. A first-approximation theoretical analysis is developed, based on the assumption that cement paste behaves as a non-Newtonian liquid, and results are compared with the experimental results.

Nomenclature

$\dot{\gamma}$	Shear strain rate in power law fluid model	CGF	Geometric factor for cement paste
γ_{zr}	Shear strain converted from ε_{zr}	d_o	Amplitude of squeeze motion
$\dot{\gamma}_{zr}$	Shear strain rate	F_N	Load in normal direction
$\dot{\varepsilon}$	Normal strain rate	g	Gravitational constant
ε_{zr}	Component of shear strain	h	Sample height
$\dot{\varepsilon}_{zr}$	Component of shear strain rate	h_o	Initial sample height
ε_{zz}	Component of normal strain	\dot{h}	Velocity of platen
η	Viscosity	k	Order of polynomial function of geometric factor for cement paste
ρ	Density of cement paste (3.2 g cm^{-3})	m	Consistency in power-law fluid model
σ_{Cav}	Calculated average normal stress of cement paste	n	Power index in power-law fluid model
σ_{Nav}	Calculated average normal stress of power law fluid	P	Pressure
σ_m	Measured normal stress of cement paste	P_a	Atmospheric pressure
σ_{zz}	Normal stress in z direction	PGF	Geometric factor for power-law fluid model
τ_{eq}	Equivalent shear stress converted from normal stress	r	Radial direction in cylindrical coordinates
τ_{rz}	Shear stress in momentum equation	R	Radius of sample
a_i	Coefficients in polynomial function of geometric factor for cement paste	s	$1/n$
B	Buoyancy force	V	Volume of the top platen submerged into cement paste
		v_r	Velocity in r direction
		v_z	Velocity in z direction
		z	Vertical direction in cylindrical coordinates

1. Introduction

The rheology of cement paste is complex, and flow properties such as the relationship between shear rate and viscosity are the subject of ongoing research. Viscometric flow conditions are usually obtained using plate–plate, cone–plate and coaxial cylinder viscometers that deform the specimen under simple shear flow. The flow has been controlled in several ways including constant shear rate [1–5], varying the shear rate [6, 7] and oscillatory shear rate [8–10], as well as controlled stress and creep [11]. The greatest advantage

of these simple geometries is the relative ease of controlling shear rate and shear stress. Rheological properties under shear flow conditions may be good indicators of the characteristics of pastes at initial stages of hydration, even though the specific values are functions of sensor geometry and are often complicated by many artefacts. Flow properties incorporate strain-rate and time-dependent behaviour under large deformations. Typically, results show that cement paste obeys a Bingham type of behaviour. Thus, a connection may be made to microstructure in that the

flocculated system yields or breaks down in the small-strain region.

Although flow under shear stress has been emphasized in the literature, there is another class of flow, known as shear-free flow, that includes elongation, squeeze and planar flows, which are important to processing. Obviously there must be shear planes associated with deformation, but these planes, oriented 45° with respect to the applied normal stress, are not stable when a specimen is squeezed between two platens, i.e. when the distance between plates is changing. Deformation, therefore, occurs by flow along planes which are constantly being disrupted and re-defined.

Other materials which have been studied extensively using squeeze flow experiments are polymer melts [12, 13], suspensions [14], composites [15, 16], asphalts [17], coal tar pitch [18] and elastomers [19, 20]. For example, the rheological behaviour of viscoelastic polymers in squeeze flow is very important in order to understand and improve polymer processing operations such as film blowing, fibre spinning, flat-film extrusion, blow moulding and vacuum forming.

Squeeze flow conditions occur during the mixing of cement paste, mortar and concrete. They are dominant factors when considering processes such as moulding and extrusion. Also, for concrete or mortar there may be a squeeze behaviour that occurs between aggregates. With few exceptions [21, 22], squeeze flow experiments have not been applied to cement paste because of the difficulties involved in controlling the experiment. Notably, the paste may flow under the influence of gravity before squeezing, and the problem of containment has not been studied. This means the rheological characteristics of cement paste have not been completely analysed.

This paper describes squeeze flow experiments that can be performed under constant stress or constant strain rate (constant velocity of top plate). Results are presented from constant-velocity experiments on cement paste. In the process of establishing an experimental technique, artefacts such as the buoyancy force, sedimentation in cement paste, the effect of the geometry of the bottom container, and the effect of friction at the interface between top plate and sample surface are considered as independent variables. The last variable is studied under two conditions at the interface, namely no-slip and slip. In the no-slip case, where the boundary layer of paste has zero velocity, squeeze flow is a coupled effect of both shear and compression. In the case of slip with a non-zero velocity condition at the interface, flow occurs along planes which fold as the distance between the plates changes. In particular, this case is equivalent to equibiaxial extensional flow. Results of constant-velocity squeeze experiments are compared with those of our constant-shear experiments [1], after normal stress and apparent normal strain are converted to an equivalent shear stress and shear strain under the assumption of a uniaxial compression test.

An analytical relationship between average normal stress and apparent strain is derived and compared

with experimental results. The derivation assumes an equibiaxial extensional flow; that is, under the condition there is no shear stress between the top plate and the sample surface.

1.1. Research significance

It must be emphasized that the experiments and analyses reported in this paper are complex and, as a result, many approximations and simplifications have been made. For example, because some of the sample squeezes out from between the plates the concept of strain, according to mechanics, cannot be applied. However, it is useful to approximate an apparent strain from the displacement of the platens, particularly at small displacements. Here apparent strain is calculated by integration of strain rate, described by the velocity field under squeeze flow. This apparent strain is called the Hencky or logarithmic strain [23]. Hencky or logarithmic strain will be used on the assumption that there is no flowing of the sample over the top plate and no friction between the plate and the sample. Even with this qualification, the results reported in this paper provide a basis for studying the shear-free flow behaviour of fresh cement paste.

2. Theoretical analysis of cement paste assuming non-Newtonian fluid behaviour

Fresh cement paste is not a Newtonian liquid since its viscosity is a function of strain rate. Such a fluid obeys a power law, proposed by Ostwald [24] and de Waele [25], and follows the functional form

$$\eta(\dot{\gamma}) = m\dot{\gamma}^{n-1} \quad (1)$$

where m and the dimensionless n are parameters commonly called the consistency and power-law index, respectively. The squeeze flow problem for a power-law fluid has been solved by Leider and Bird [26]. Cylindrical coordinates (taking $v_r = v_r(r, z)$, $v_z = v_z(z)$ and $p = p(r)$, and discarding all internal terms) are placed midway between the discs as shown in Fig. 1. In addition to the assumption of a quasi-steady state, a condition of no-slip at the interface between paste and sensor is invoked. In the light of these simplifying assumptions, the continuity equation and momentum equation reduce to

$$\frac{1}{r} \left(\frac{\partial(rv_r)}{\partial r} \right) + \frac{\partial v_z}{\partial z} = 0 \quad (2)$$

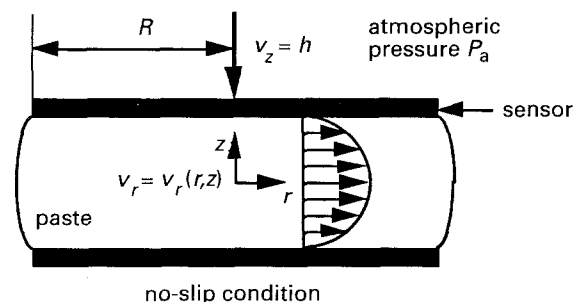


Figure 1 Geometry of squeeze flow of non-Newtonian fluid.

and

$$\frac{\partial p}{\partial r} + \frac{\partial \tau_{rz}}{\partial z} = 0 \quad (3)$$

From the no-slip condition, the following boundary conditions are invoked:

$$v_r = 0 \quad \text{at } z = h \quad (4)$$

$$\tau_{rz} = 0 \quad \text{at } z = 0 \quad (5)$$

and

$$v_r = \frac{h^{1+s}}{1+s} \left[\frac{-1}{m} \left(\frac{dp}{dr} \right) \right]^s \left[1 - \left(\frac{z}{h} \right)^{1+s} \right] \quad (6)$$

where $s = 1/n$. The pressure profile is calculated with the following boundary conditions: $p = P$ at $r = r$ and $p = P_a$ at $r = R$. It is expressed by

$$P = P_a + m \frac{(2+s)^n}{2^n(n+1)} \left(\frac{(-\dot{h})^n R^{1+n}}{h^{1+2n}} \right) \times \left[1 - \left(\frac{r}{R} \right)^{1+n} \right] \quad (7)$$

where P_a is the atmospheric pressure. The total instantaneous force that must be applied to the disc at $z = h$ is obtained from Equation 7 by integrating P over the surface of the disc. This results in the expression

$$F_N = m\pi \frac{(2+s)^n}{2^n(3+n)} \left(\frac{(-\dot{h})^n R^{3+n}}{h^{1+2n}} \right) \quad (8)$$

The average normal stress of a non-Newtonian fluid at the plate can then be calculated:

$$\sigma_{Nav} = \frac{F_N}{\pi R^2} = m \frac{(2+s)^n}{2^n(3+n)} \left(\frac{(-\dot{h})^n R^{1+n}}{h^{1+2n}} \right) \quad (9)$$

If the definition of logarithmic strain rate is invoked, then the above equation is expressed by

$$\sigma_{Nav} = m\dot{\epsilon}^n \frac{(2+s)^n}{2^n(3+n)} \left(\frac{R}{h} \right)^{1+n} \quad (10)$$

The parameters m and n are obtained by a trial and error method using Equation 10, giving

$$m = 700 \quad n = 0.2 \quad (11)$$

From Equation 10, a geometric factor for power-law fluids (PGF), which shows the effect of the dimensionless geometric parameter, R/h , in squeeze flow can be defined:

$$PGF = \left(\frac{R}{h} \right)^{1+n} \quad (12)$$

From Equation 10, and setting $\sigma_m = \sigma_{Nav}$, geometric factor for fresh cement paste (CGF) is written as a polynomial function of R/h :

$$CGF = \sum_{i=0}^k a_i \left(\frac{R}{h} \right)^i \quad (13)$$

where i includes the parameter n , a_i are constants obtained from curve-fitting to experimental results and k is taken as 3rd order in this experiment. The analytical result for normal stress using the geometric

factor for cement paste is

$$\sigma_{Cav} = m\dot{\epsilon}^n \frac{(2+s)^n}{2^n(3+n)} \sum_{i=0}^3 a_i \left(\frac{R}{h} \right)^i \quad (14)$$

3. Experimental procedure

A typical Type I Portland cement was used, and the cement paste was prepared by mixing cement and water in a Hobart mixer. The water/cement ratio by weight was 0.4 for all experiments. Mixing intensity and time of mixing were 30 r.p.m. and 5 min, respectively.

As shown in Fig. 2, the apparatus for measuring rheological properties consists of a top plate connected to a load cell and a bottom container. The diameter of the top plate was 203.2 mm, and the diameter of the bottom container was one of the following: 210, 270, 360 and 610 mm, depending on the experiment. In contrast with a conventional squeeze flow experiment in which the diameters of platens are much larger than the sample, a bottom container was used to contain the fresh cement paste and the top plate penetrated the contained paste.

Cement paste was poured into the bottom container and adjusted to a given initial sample height by adjusting the weight of the cement paste; here, initial sample heights were 18, 36, 54 and 72 mm. The bottom container and cement paste were placed on the bottom plate of the servohydraulic machine. Then the top plate was lowered. The interface between the top plate and the sample surface was controlled by setting the initial load within the range -0.1 to -0.5 N (compression). The squeeze displacements were 1, 5 and 10 mm and the squeezing period was 120 s.

The load and displacement of the sample were measured with a load cell and a linear variable differential transformer (LVDT). The load cell measured only the normal component of the load, and the average normal stress was obtained by dividing the load by the area of the top plate. The capacity of the load cell was 1000 N. Experiments were performed under

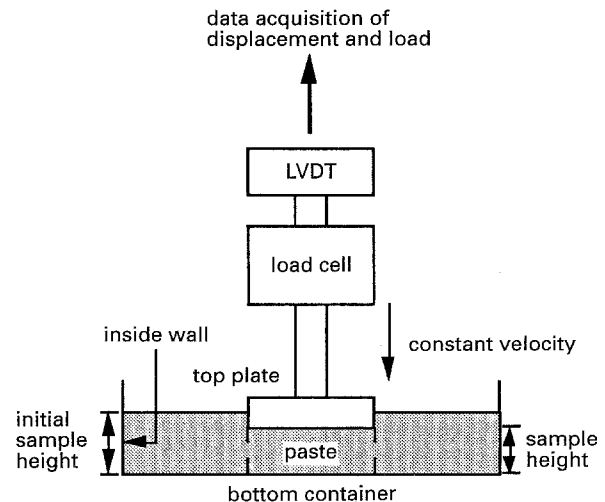


Figure 2 Schematic diagram of squeeze flow experimental system. Initial sample height 18, 36, 54 or 72 mm; constant velocity 0.0083, 0.0417 or 0.0833 mm s⁻¹.

TABLE I Experimental conditions for constant-velocity flow experiments

Initial sample height (mm)	Amplitude of ramp signal (mm)	Average logarithmic strain rate (s^{-1})
36	1	0.000234
	5	0.00126
	10	0.00275
18	1	0.0048
	5	0.00275
	10	0.0075

constant squeeze rate; that is, a constant lowering velocity of the top plate. The apparent normal strain is expressed by using the definition of logarithmic strain

$$\varepsilon(t) = \ln\left(\frac{h(t)}{h_0}\right) = \ln\left(\frac{h_0 - d_0(t)}{h_0}\right) \quad (15)$$

where h is the sample height, d_0 the squeeze displacement and h_0 the initial sample height. The apparent normal strain rate is given by

$$\dot{\varepsilon}(t) = \frac{d\varepsilon}{dt} = \frac{\dot{h}}{h(t)} \quad (16)$$

where \dot{h} is the constant velocity of the top plate. For analysis of these results, the average normal strain rate is obtained as the arithmetic mean of initial and final normal strain rates. Table I shows the experimental conditions for the constant-velocity squeeze flow experiments.

4. Artefacts related to a squeeze experiment

In a conventional squeeze experiment, the sample is loaded between top and bottom plates that have the same area. In this geometry the sample deforms in the radial direction by squeezing vertically. Normally the samples cannot flow under their own weight; however, cement paste can flow and therefore it must be contained, introducing the unknown influence of the restricting wall of the bottom container. Thus the effect of varying the ratio of the diameter of the top plate to that of the bottom container must be established. This was done by using a top plate of constant diameter and four bottom containers with different diameters. Another consideration was the buoyancy force of the top plate as it penetrates the paste. Finally, friction between the top plate and the surface of the sample is important because it causes a shear stress at the interface during deformation. These potential problems had to be investigated before squeeze flow experiments could be interpreted.

4.1. Effect of the dimensions of the container

The effect of the diameter of the bottom container on the peak load, under otherwise identical experimental conditions, is shown in Fig. 3. If the bottom container has nearly the same diameter as the top plate, then the cement paste overflows the wall of the bottom con-

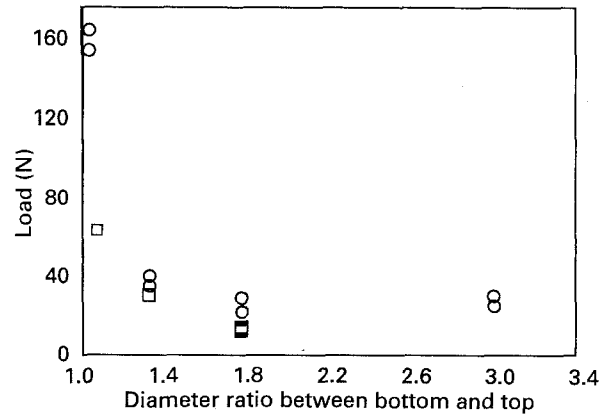


Figure 3 Effect of dimension of the bottom container on the peak load: sample height (○) 18 mm, (□) 36 mm.

tainer during the test. Larger diameters of the bottom container prevent this, although the sample extends in the radial direction to the wall. This means that there is a lower limit for the ratio of the diameters of the top plate and bottom container for which meaningful experiments can be performed. In this experiment it was found that the effect of a repulsive force from the wall can be neglected at a diameter ratio larger than 1.7, as suggested by the constant loads shown in Fig. 3. Therefore a bottom container diameter of 36 cm was adopted for use in the main experiment.

4.2. Effect of buoyancy force on experiment results

During the squeezing motion of the top plate an upward force is generated by the buoyancy of the top plate as it enters the paste. The buoyancy force B can be expressed as

$$B = \rho Vg \quad (17)$$

where ρ is the density of cement paste and V is the volume of the top plate submerged in cement paste. In our experiment, this effect was computed to be approximately 15% of the measured load. In other words, the measured load is about 15% larger than that at the top interface between plate and paste.

4.3. State of friction between top plate and surface of sample

The effect of friction at the interface between top plate and surface of sample was investigated by using motor oil (SAE-30), Teflon and sandpaper on both top plate and bottom container. Before doing these experiments, cement paste was placed on a plate that was coated with either a lubricant or sandpaper and tilted with respect to the horizontal. The Teflon coating allowed the paste to slide better than did the motor oil, so, Teflon was used to approach a frictionless condition. Sandpaper produced sticking condition at the interface.

Fig. 4 shows a plot of normal stress versus apparent strain (as defined by displacement) at constant velocity of the top plate for the two interfacial conditions. The

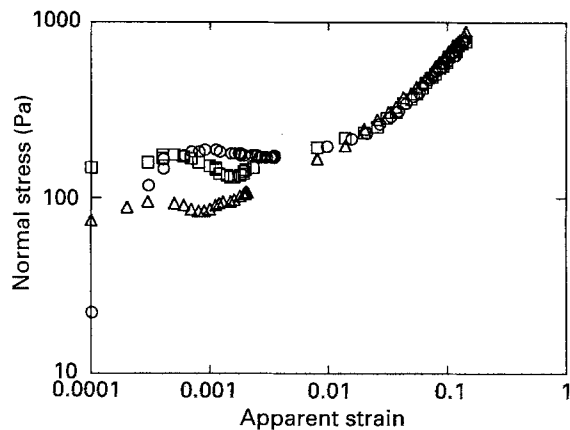


Figure 4 Effect of friction state on normal stress versus apparent strain: (○) lubricant (Teflon spray), (□) sandpaper, (△) non-lubricant.

initial sample height was 36 mm and the squeeze displacement was 5 mm. In the case of sandpaper the results show that the highest load occurs initially, due to friction between plate and surface of sample. By comparing these results with those from the zero-friction experiments, it is apparent that as the squeezing of the sample progresses, the influence of the state of friction at the interface becomes less pronounced. In other words there is not much difference between lubricated and non-lubricated conditions except at the initial stage of compression. There is no way of measuring directly the shear stress due to friction; therefore, it is difficult to analyse an experiment in which friction plays a large role. The following results are obtained from experiments that used Teflon at the interface.

5. Results and discussion

5.1. Cement paste

The average normal stress is related to the apparent strain for various average apparent strain rates (produced by varying initial sample heights or squeeze displacements) as shown in Fig. 5. The curves are approximately S-shaped, and can be divided into three regimes regardless of the apparent strain rate. There is much scatter of stress for small apparent strain rate, due in part to the reduced accuracy of the load cell at small loads.

Region I shows a linear relationship between stress and apparent strain. The range of region I increases with increasing apparent strain rate. Thus, cement paste exhibits a linear elastic region under squeeze flow conditions as well as under shear flow [1].

Region II is nearly flat, i.e. the stress increases only by a small amount with increasing apparent strain, or in other words cement paste deforms plastically. This is in contrast to the results from shear flow experiments, where the cement paste exhibited a structure breakdown after a yield point of greater stress than that needed to sustain region II [1].

In region III, at large apparent strains, the normal stress increases with increased apparent strain. This increasing stress is in contrast with a continuous structural breakdown observed in shear flow experi-

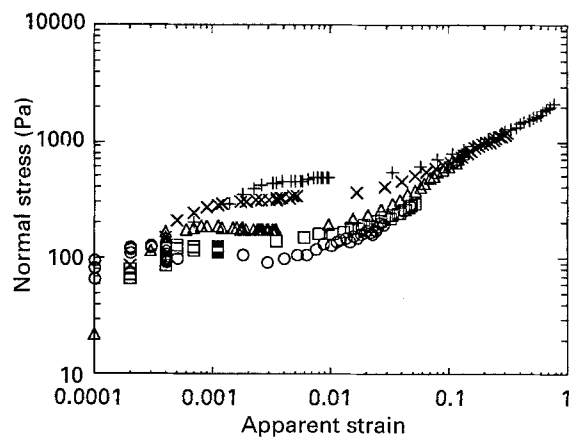


Figure 5 Average normal stress versus strain for various average apparent strain rates: (○) $0.000\ 234\ \text{s}^{-1}$, (□) $0.000\ 48\ \text{s}^{-1}$, (△) $0.001\ 26\ \text{s}^{-1}$, (×) $0.002\ 75\ \text{s}^{-1}$, (+) $0.0075\ \text{s}^{-1}$.

ments [1]. The location of the beginning of region III depends on apparent strain rate, occurring at lower values of apparent strain when the apparent strain rates are smaller. Regions II and III show that the behaviour of cement paste differs under different experimental conditions, and indeed the results from shear flow and squeeze flow are opposite at large apparent strains, i.e. strain softening (shear flow) or strain hardening (squeeze flow).

5.2. Mechanism for strain hardening

Possible mechanisms for the strain-hardening behaviour under squeeze flow were investigated by the following experiments: (i) superplasticizer was added to paste, and (ii) tests were carried out using a combination of compression, rest (and associated relaxation) and tension. A superplasticizer reduces the viscosity and therefore should alter region III if it is a material property. Tensile stress is applied by increasing the distance between the plates and, once again, this will provide insight into any geometric effects of strain hardening, i.e. whether strain hardening is due to the plates approaching each other.

The effect of a superplasticizer on the relationship of stress to apparent strain is shown in Fig. 6. Superplasticizer (ASTM C-494 type A) was added at 1% by weight of cement. The data are plotted on linear scales since strain hardening occurs at large deformation, and also because there is much scatter of measured stress at small strain due to the limits of accuracy of the load cell. The results show that cement paste exhibits strain-hardening behaviour both with and without superplasticizer, but the gradient of the increasing stress is reduced by the addition of a superplasticizer. This means that strain hardening is caused, at least in part, by the geometry of the specimen. Indeed, because paste is being squeezed out of the region between the plates, the concept of strain breaks down completely at large displacements.

The second group of experiments cycled specimens through compression, rest and tension, each for a period of 120 s. Fig. 7 shows a plot of normal stress as a function of time for three 120 s periods. The normal stress increases during compression of the top

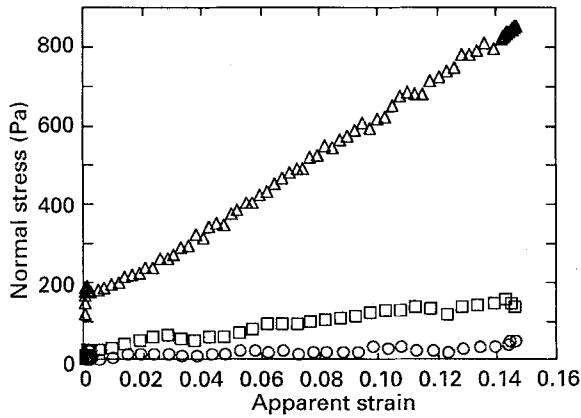


Figure 6 Effect of superplasticizer on stress versus apparent strain: (Δ) none, (\square) 0.3% of cement weight (15 g), (\circ) 1% of cement weight (50 g).

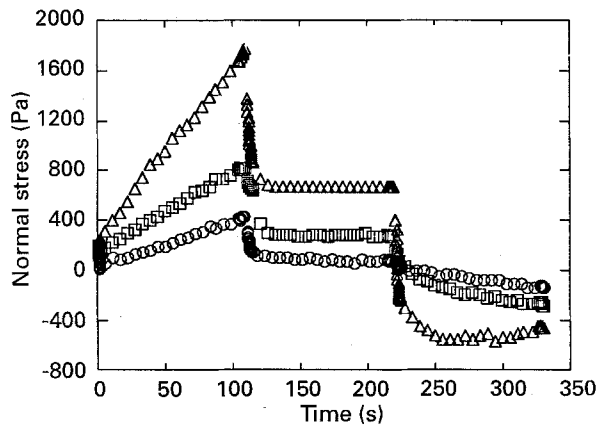


Figure 7 Stress versus time under compression, rest and tension cycle of top plate. Ratio of squeezing amplitude (mm) to initial sample height (mm): (\circ) 5.36, (\square) 5.18, (Δ) 10.18.

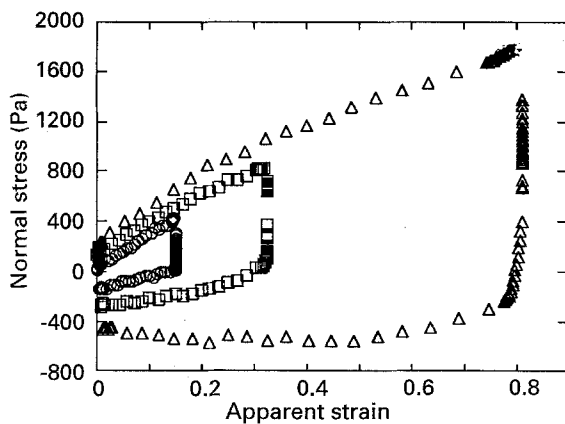


Figure 8 Stress versus apparent strain under compression, rest and tension cycle of top plate. Ratio of squeezing amplitude (mm) to initial sample height (mm): (\circ) 5.36, (\square) 5.18, (Δ) 10.18.

plate, and it drops off as soon as the rest period begins. After the drop, the normal stress is constant, i.e. it is a residual stresses. Fig. 8 shows the normal stress as a function of apparent strain under the same condition as shown in Fig. 7. The curves show a similar type of hysteresis loop regardless of experimental conditions. During unloading, or during tension, cement paste shows as elastic behaviour before the beginning of its plastic behaviour, although it has a gentle com-

pared with that of the compression curve. This may mean that the packing of cement particles changes during compression and tension. The peak stress at the end of the unloading, or tension step is small compared with that of compression step.

5.3. Equivalent shear stress

A comparison of these results with results from shear flow techniques may be attempted by converting normal stress and apparent strain to an equivalent shear stress and strain, using the assumption of uniaxial compression. Once again there are many assumptions involved in this analysis. Perhaps the most notable is that difficulties associated with paste flowing out from between the plates and into the container, i.e. difficulties associated with the definition of strain, are being ignored. Also end-effects are being greatly simplified in our analysis. However, some insight may be gained from the analysis, particularly for small displacement. The equivalent or resolved shear stress, τ_{eq} , is obtained using Mohr's circle.

$$\tau_{eq} = \frac{1}{2} \sigma_{zz} \quad (18)$$

Similarly, if the Poisson's ratio of fresh cement paste is assumed to be 0.5 from the volume constancy (in other words, if an equibiaxial extensional flow is assumed), the relationship between apparent shear strain and apparent normal strain components is also obtained using Mohr's circle.

$$\epsilon_{zr} = \frac{3}{4} \epsilon_{zz} \quad (19)$$

From the relationship $\gamma_{zr} = 2\epsilon_{zr}$, the converted shear strain, γ_{zr} , is given as

$$\gamma_{zr} = \frac{3}{2} \epsilon_{zz} \quad (20)$$

and the converted shear strain rate, $\dot{\gamma}_{zr}$, is

$$\dot{\gamma}_{zr} = \frac{3}{2} \dot{\epsilon}_{zz} \quad (21)$$

Based on this analysis, Fig. 9 shows plots of shear stress versus shear strain rate, obtained from shear flow experiments in our earlier work [1], and equivalent shear stress versus equivalent shear strain rate obtained from squeeze flow experiments. The shear and equivalent shear rates of large value produce stresses of high value. The experimental technique apparently determines whether or not cement paste shows strain softening or strain hardening behaviour. In other words, cement paste may have a different deformation process caused by shear than by squeeze flow.

A comparison of flat (squeeze flow) and yield (shear flow) stresses as a function of strain rate is shown in Fig. 10. The values of data points were obtained as follows. Shear flow experiments [1] were performed for shear strain rates of 0.1, 0.2, 0.4, 0.8, 1.6 and 6.4 s^{-1} . Squeeze flow experiments, however, were performed at very small equivalent shear strain rates of

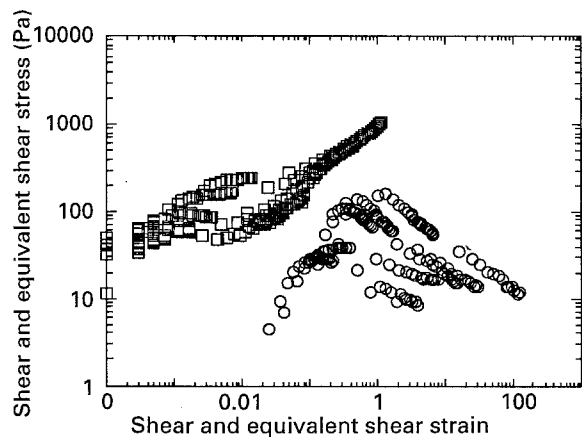


Figure 9 Comparison of plots of stress versus apparent strain for (○) shear and (□) squeeze experiments. Squeeze experiments: equivalent shear rates 0.000 35, 0.000 72, 0.004 12, 0.001 89, 0.011 25 s⁻¹. Shear experiments: shear rates 0.2, 0.4, 0.8, 1.6, 6.4 s⁻¹. High values of rate represent high values of stress.

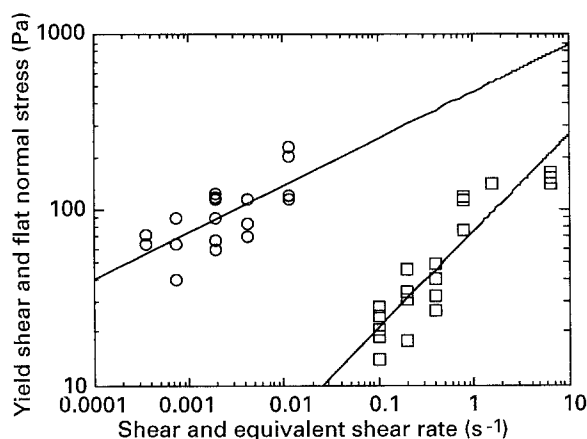


Figure 10 (□) Yield shear and (○) flat normal stresses as a function of apparent strain rate. Power laws: flat stress $493.6 \dot{\gamma}_{eq}^{0.275}$, shear stress $76 \dot{\gamma}^{0.55}$.

0.000 35, 0.000 72, 0.001 89, 0.004 12 and 0.011 25 s⁻¹. The equivalent yield shear stresses are taken as the stresses that are at the boundary between regions I and II in Fig. 5. The flat normal stresses are determined at normal apparent strain value intermediate between the beginning and ending of region II, which may be interpreted as a yield stress from squeeze experiments.

These two stresses are modelled by power-law equations as shown in Fig. 10 for shear strain rate and equivalent shear strain rate, respectively. If these materials and tests were showing material behaviour, the yield shear stress and the equivalent flat shear stress would lie on the same line and have the same power-law index and coefficient. However, the results show different power-law indices and coefficients: the power-law indices differ by approximately a factor of two, and the power-law coefficients differ by a factor of six. Either different properties are being measured by the different experiments, or one or the other of the results is fallacious.

5.4. Comparison of analytical and experimental results

The rheological behaviours in regions II and III in Fig. 5 are analysed using non-Newtonian fluid beha-

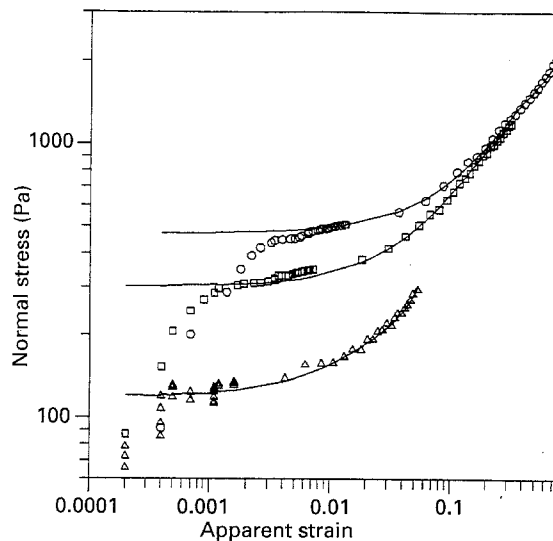


Figure 11 Comparison of measured and calculated stresses using a geometric factor for cement paste. Initial sample height = 18 mm. Average apparent strain rate (measured): (Δ) 0.000 49 s⁻¹, (□) 0.0032 s⁻¹, (○) 0.0104 s⁻¹; (—) calculated from Equation 14.

viour under squeezing motion. Fig. 11 shows a comparison of measured and calculated stresses using Equations 14 according to average apparent strain rates with an initial sample height of 18 mm. There is a good agreement, suggesting that at large strain the “hardening” is due to non-Newtonian fluid behaviour of cement paste. However, the initial apparent strain region apparently does not follow non-Newtonian fluid behaviour. Thus, there is a limitation to the non-Newtonian fluid model at very small apparent strains. Perhaps at very small apparent strains cement paste behaves like a solid. Although there is good agreement, the analysis must be interpreted with caution.

6. Conclusion

Normalized results from squeeze flow experiments do not agree with those from shear flow experiments. The difference between shear and squeeze is, perhaps, due to the different geometry of deformation of sample. In spite of the difficulties mentioned in the section on the relation of artefacts to squeeze experiments, an experimental technique for measuring the squeeze flow characteristics of cement paste has been developed. It provides important new information about the rheology of cement paste under conditions where stable shear planes are suppressed. The results may be relevant to processes such as extrusion.

Theoretical and experimental analyses of the rheological characteristics of cement paste under squeeze flow conditions are discussed. This behaviour is divided into elastic (at small apparent strain), plastic (after yielding) and strain hardening (at large apparent strain) regions. The latter region is similar to that often exhibited by solid-like deformation behaviour. On the other hand, strain hardening at large apparent strain is analysed by considering the paste to be a non-Newtonian fluid obeying a power law. This analysis shows good agreement between experiment and the-

ory, indicating that the strain hardening is a consequence of the geometry of the measurement process. These results indicate that cement paste, at large deformation, behaves like a non-Newtonian fluid.

Acknowledgements

The authors would like to express their appreciation to Concrete Technology Corporation of Santa Barbara, California, for instrumentation and financial support of this work, and the National Science Foundation Center for Advanced Cement Based Materials, grant DMR-88080432. It is with regret that we report that Professor Lewis Erwin died during the final stages of this research.

References

1. B. H. MIN, L. ERWIN, and H. M. JENNINGS, *Ceram. Trans.* **16** (1990) 337.
2. *Idem*, *Korean J. of Rheol.*, in press.
3. G. H. TATTERSALL, *Nature* **175** (1955) 166.
4. R. LAPSIN, *Cemento* **4** (1982) 243.
5. W. VOM BERG, in Proceedings of 8th International Congress on Rheology, Vol. 3 (Plenum, New York, 1980) p. 665.
6. I. ODLER, T. BECKER and B. WEISS, *Cemento* (1978) 303.
7. P. F. G. BANFILL, *Mag. Concr. Res.* **33** (1981) 37.
8. T. E. R. JONES, G. BRINDLY and B. C. PATEL, in "Hydraulic Cement Pastes: Their Structure and Properties", Proceedings of Conference, University of Sheffield, 1976, p. 135.
9. A. R. CUSEN and J. HARRIS, in Proceedings of RILEM, on "Fresh concrete; important properties and their measurements, Sem". Leeds, England, 1973. Vol. 1 (Dept. of Civil Engng. University of Leeds, Leeds, England, 1973) p. 2.8.1.
10. T. M. CHOW, L. V. McINTIRE, K. R. KUNZE and C. E. COOKE, *SPE Prod Engng* **3**(4) (1988) 543.
11. P. F. G. BANFILL and D. R. KITCHING, in Proceedings of International Congress on Rheology of Fresh Cement and Concrete, edited by P. F. G. Banfill (University Press, Cambridge, 1991) p. 125.
12. G. J. DIENES and H. F. KLEMM, *J. Appl. Phys.* **17** (1946) 458.
13. G. J. DIENES, *J. Coll. Sci.* **2** (1947) 131.
14. R. J. GRIMM, *AIChE J.* **24** (1978) 427.
15. K. S. GANDHI and R. BURNS, *Trans. Soc. Rheol.* **20** (1976) 489.
16. R. J. SILVA-NIETTO, B. C. FISHER and A. W. BIRLY, *Polym. Engng Sci.* **21** (1981) 499.
17. E. J. DICKENSON and H. P. WITT, *Trans. Soc. Rheol.* **13** (1969) 485.
18. A. N. GENT, *Br. J. Appl. Phys.* **11** (1960) 85.
19. M. J. FOSTER, *J. Appl. Phys.* **26** (1955) 1104.
20. S. H. CHATRAEI, C. W. MACOSKO and H. H. WINTER, *J. Rheol.* **25** (1981) 433.
21. A. TERYTYEV and G. KUNNOS, in Proceedings of International Congress on Rheology of Fresh Cement and Concrete, edited by P.F.G. Banfill (Cambridge University Press, Cambridge, 1990) p. 93.
22. M. REINER, in "Rheology", Vol. 3, edited by F. R. Eirich (Academic, New York, 1960) p. 351.
23. R. B. BIRD, R. C. ARMSTRONG and O. HASSAGER, "Dynamics of Polymeric Liquids", Vol. 1, (Wiley, New York 1977) p. 429.
24. W. OSTWALD, *V. Kolloid-Z.* **36** (1925) 99.
25. A. De WAELE, *Oil & Color Chem. Assoc. J.* **6** (1923) 23.
26. P. J. LEIDER and R. B. BIRD, in "Industrial Engineering Chemical Fundamentals", Vol. 13 (American Chemical Society, Washington, 1974) p. 336.

Received 28 July
and accepted 26 August 1993